Article

Potential of Digital Sensors for Land Cover and Tree Species Classifications – A Case Study in the Framework of the DGPF-Project

Lars T. Waser, Birmensdorf, Switzerland, Sascha Klonus, Manfred Ehlers, Osnabrück, Meinrad Küchler, Birmensdorf, Switzerland & András Jung, Halle

Summary: The study is intended as a contribution to assessing the value of digital image data for semi-automatic analysis of classified land cover and tree species and was carried out in the framework of the DGPF-project. Sensor specific strengths of ADS40-2nd, Quattro DigiCAM, DMC, JAS-150, Ultracam-X, and RMK-Top15 cameras and weakness for classification purposes are presented and shortly discussed. The first approach is based on a maximum likelihood method in combination with a decision tree and produces 13 land cover classes. The second approach is based on logistic regression models and produces eight tree species classes.

The classified images were visually assessed and quantitatively analyzed. The accuracy assessment reveals that in both approaches similar classification results are obtained by all sensors with overall Kappa coefficients between 0.6 and 0.9. However, a real sensor comparison was not possible since the image data was acquired at different dates. Thus, some variations in the classification results are due to phenological differences and different illumination and atmospheric conditions. It is planned for the future that the classifications of the first approach will be adjusted to the characteristics of each sensor. In the second approach, further work is needed to improve distinguishing non-dominant, small and partly covered deciduous tree species.

Zusammenfassung: *Potenzial digitaler Sensoren zur Klassifizierung der Landbedeckung und Baumarten – eine Fallstudie im Rahmen des DGPF-Projektes*. Anhand der Bilddaten aus den Kamerasystemen ADS40-2nd, Quattro DigiCAM, DMC, JAS-150, Ultracam-X, und RMK-Top15 wurden zwei Klassifikationsverfahren (Maximum Likelihood und logistische Regression) getestet. Dabei wurden sensor-spezifische Eigenschaften erläutert, sowie die Stärken und Schwächen der einzelnen Systeme aufgezeigt.

Die Resultate wurden visuell und quantitativ bewertet. Direkte Sensorvergleiche erwiesen sich dabei als schwierig, da zum Aufnahmezeitpunkt der einzelnen Bilddaten sowohl eine unterschiedliche Vegetationsentwicklung wie auch Unterschiede in den Beleuchtungs- und atmosphärischen Verhältnissen vorherrschten. Quantitative Analysen zeigen, dass sich mit jedem Kamerasysteme sehr ähnlich gute Resultate erzielen liessen. Das erste Verfahren zeigt für 13 Landnutzungsklassen Kappa Koeffizienten von gut 0,6 bei allen verwendeten Systemen. Allerdings unterscheidet sich die Genauigkeit der einzelnen spezifischen Klassen wie Mais oder Kartoffeln für die unterschiedlichen Kameras. Hierzu soll in weiteren Analysen das Klassifikationsverfahren an die jeweiligen Kameras angepasst werden. Für das zweite Verfahren liegt der Kappa Koeffizient für 8 Baumarten zwischen 0,7 und 0,9. Bei diesem Verfahren soll in zukünftigen Analysen die Genauigkeit der Erkennung von nicht dominanten, kleinen und teilweise verdeckten Baumarten erhöht werden.

1   Introduction

This paper compares different aerial cameras for land cover classification purposes. It was carried out in the framework of the project of the German Society for Photogrammetry, Remote Sensing and Geoinformation (DGPF). An overwiev and test design of this project is given in this issue (Cramer 2010). In the DGPF-project "Evaluation of digital aerial cameras" a special interest group "Thematic Analysis" was initiated within the radiometry working group. The objective of this group is the comparison of the different aerial cameras in terms of information extraction.

While there are many articles related to the radiometric comparison between different aerial cameras (Markelin et al. 2006; Hoonkvaara et al. 2009), there are only a few articles related to a comparison of the classification accuracy between different aerial cameras. E. g. Ehlers et al. (2007) used different supervised classification methods to compare DMC, UCD and ADS40 data. Rosso et al. (2008) compare different spectral curves of specific plant species from DMC, UCD and ADS40 data. Further articles are related to this project (Klonus 2009; Klonus et al. 2009).

The focus of the Institute for Geoinformatics and Remote Sensing (IGF) at the University of Osnabrück in this article is on an entire land cover classification whereas the group Pattern Recognition and Photogrammetry at the Swiss Federal Research Institute (WSL) focusses on the classification of forest area and different tree species.

The general objective of an image classification is the automatic allocation of all pixels to land cover classes or specific themes. The grey value of each pixel is the numeric base for this allocation (Lillesand & Kiefer 1994). According to Jensen (2005) the multispectral classification can be processed using one or more of the following approaches:

- algorithms based on parametric and non-parametric statistics
- supervised and unsupervised classification algorithms
- the use of hard or soft classifications (Fuzzy)
- pixel and object based classification algorithms

- or hybrid approaches.

None of these classification methods is superior to another. The most appropriate classification strategy depends on different parameters such as the biophysical characteristics of the research area, the homogeneity of the remote sensing data and the "a priori" knowledge (Jensen 2005). Even a standard algorithm, such as the maximum likelihood, could produce better results than modern algorithms such as ANN (artificial neural networks) (Erbek et al. 2004) or boosting (Bailly et al. 2007). An overview of classification algorithms is given in (Lu & Weng 2007).

According to Scott et al. (2002), modern regression approaches are particularly useful for modelling the spatial distribution of tree species and communities. When analyzing the relationship between categorical dependent variables and remotely sensed data logistic regression models are very powerful. Thus, regression analyses with explanatory variables derived from high-resolution remote sensing data seem very promising for the second part of this article – modelling tree area and tree species. Some recent forest research has focused on integrating multisensor data to estimate forest area (Wang et al. 2007; Waser et al. 2008a), forest composition and tree species (Heinzel et al. 2008). But only few studies have already shown that optical digital airborne data have also been opened up new opportunities for tree species classification: The data are recorded by frame-based sensors, e. g. DMC (Holmgren et al. 2008), Ultracam-X (Hirschmugl et al. 2007) or line-scanning sensors, e. g. ADS40 (Waser et al. 2008b), which provide stereo-overlap of up to 90 % or entire image strips with higher radiometric resolution.

The main objective of this article was to show the potential of frame-based camera systems (DMC, Quattro DigiCAM, Ultracam-X), two line scanning systems (ADS40-2nd, JAS-150) and a classical analogue camera (RMK-Top15) for two different classification approaches. Sensor specific strengths and weakness for classification purposes will be briefly investigated and emphasis was placed on objectivity and not only on accuracy of classification.

2 Material

2.1 *Study Area*

The DGPF-project study area is located about 20 km north-west of Stuttgart/Germany in a hilly area providing several types of vegetation and land use, mostly rural area with smaller forests and villages, quite steep vineyards and some quarries.

To save processing time, two smaller areas of the DGPF-project study area were chosen as test sites for the classification algorithms (cf. Fig. 1). To collect ground truth data for interpretation and classification of the recorded scenes different field trips were carried out. Both particular locations were chosen, because they present the highest heterogenity of our study area and include artificial and natural areas. In test site 1 nearly all crops were represented, whereas test site 2 is characterized by different forest types.

Test Site 1

Test site 1 is located between the villages Vaihingen and Rosswag. And is approx. 2 km^2 in area. The terrain is mostly characterized by agricultural fields in the South and vineyards in the norhern part. The area is crossed by a forest, a stone quarrel and the river Enz.

The first field survey was carried out on 12th and 13th of April 2008 and arranged by the company EFTAS of Münster. Summer and winter crops as well as different objects in the settlements were recorded. The entire spectrum of field crops (nearly 85 % of the area) and tree species in selected forest areas were recorded between 20th and 22nd of June 2008 by experts from the University of Düsseldorf (HHUD). The field survey of the University of Osnabrück was carried out during the first flights of the digital aerial cameras between 27th and 31st of July 2008. The data was collected for selected areas and updated from the HHUD. During the recording of the Ultracam-X and AIC images another field survey from 10th of September to 3rd of October 2008 was carried out by the company C+B Technik GmbH. The mapping also included the field crops in autumn. The last field survey was carried out by experts of the University of Düsseldorf from 18th to 19th of October 2008. The field crops from the first field trip were updated and the current field crops were recorded. Prior to digitizing and storing the field information in vector files all field surveys were documented with photographs in the directions North, South, East and West for the different field crops.

Fig. 1: DMC RGB Orthoimage of test sites 1 and 2.

1. Maple, 2. Beech, 3. Ash, 4. Poplar, 5. Oak, 6. Willow, 7. Norway spruce, 8. Scots pine

Fig. 2: Examples of the 8 sampled tree species in test site 2 as they appear in the ADS40-2nd imagery (RGB and CIR).

Test Site 2

Test site 2 is located in the southern part of the village Rosswag and is approx. 1.75 km^2 in area. The terrain varies (forest slopes and flat areas along the river Enz) with mixed land cover and forest. The altitude ranges from 240 m to 410 m a.s.l. The forest area covers approx. 0.7 km^2, and is mostly characterized by mixed forest (approx. 80 %) and riverside woodland (approx. 20 %). The dominating deciduous tree species are ash (*Fraxinus sp.*), beech (*Fagus sp.*), poplar (*Populus sp.*) and willow (*Salix sp.*) and less frequently maple (*Acer sp.*) and oak (*Quercus sp.*). Norway spruce (*Picea Abies*) and Scots pine (*Pinus sylvestris*) are the main coniferous trees. The ground truth data to validate the different outputs was collected in the natural environment to be representative for test site 2. For the validation of the tree cover (forest area), two types of samples were distinguished (tree area / non tree area) and a total number of 2 × 60 samples were digitized from the four input orthoimages. To determine the eight main tree species, a ground survey visiting 240 trees was carried out on 10th of June 2009. Typical examples of each tree species as seen in the ADS40-2nd RGB and CIR images are shown in Fig. 2. This information was used to calibrate and validate the logistic regression models.

2.2 *Optical Sensors*

In the framework of the DGPF-project, data was recorded by nine different aerial cameras: DMC, ADS40-2nd, JAS-150, Ultracam-X, RMK-Top15, Quattro DigiCAM, AIC-x1, AIC-x4 and DLR 3K-Kamera. Most of the cameras (DMC, RMK-Top15, ADS40-2nd, Quattro DigiCAM) recorded the data on 06th of August 2008, whereas the data from JAS-150, Ultracam-X, AIC-x1, was recorded at the beginning of September. The data of the Canon 3K camera from DLR, which was recorded on 15th of July 2008 was not used in this study due to large seasonal differences. Tab. 1 gives an overview of the characteristics of the six camera systems for which the data was available on time and therefore have been tested for classification of land cover and tree species. Allthough the image data was recorded with a ground sampling distance (GSD) of 8 and 20 cm by all cameras, a GSD of 20 cm was considered to have sufficient terrain detail for our study.

In terms of spectral characteristics DMC and JAS-150 recorded the data in the visible red, green and blue and in the near-infrared (NIR) range. Ultracam-X recorded the data in the same wavelengths, but provided only the visible bands for the test sites. The Quattro DigiCAM recorded the data only in the three visible bands: red, green and blue. For the RMK-Top15 camera the NIR, red and green data was available at 20 cm resolution. To use

Tab. 1: Summary of characteristics of the image data used in this study.

Sensor	ADS40-2nd	DMC	RMK-Top15	Quattro DigiCAM	JAS-150	Ultracam-X
Used in test site	2	1,2	1	1	1,2	1,2
Acquisition date	06/08/2008	06/08/2008	06/08/2008	06/08/2008	09/09/2008	11/09/2008
Spectral resolution (nm)	RGB+NIR B: 428-492 G: 533-587 R: 608-662 NIR: 833-887	RGB+NIR B: 429-514 G: 514-600 R: 600-676 NIR: 695-831	RG+NIR B: -- G: -- R:-- NIR:--	RGB B: 400-540 G: 480-600 R: 580-660 NIR: --	RGB+NIR B: 440-510 G: 520-590 R: 620-680 NIR: 780-850	RGB+NIR B: 400-580 G: 500-650 R: 590-675 NIR:--
Spatial resolution	20 cm	20 cm	20 cm (RGB: 8 cm)	20 cm	20 cm	20 cm
Radiometric resolution	12 bit	12 bit	--	14 bit	12 bit	>12 bit

at least three different bands of each sensor DMC, JAS-150, DigiCAM and Ultracam were studied together using the RGB bands. RMK-Top15 was also included but using the band combination RGN (red, green, near infrared). The objectivity of our comparisons is slightly reduced by this compromise. The usage of the NIR band of the RMK-Top15 has the advantage that the entropy is substantial higher than it is when only using optical bands, because the RGB bands have a higher correlation between each other and therefore lower entropy. Additionally, the main advantage of the NIR information is the better detection of plants (ALBERTZ 2001). Concerning the four band classifications only ADS40-2nd, DMC and JAS-150 data could be compared since only for these three cameras all four channels were available.

2.3 *LiDAR DTM and DSM*

In addition to the image data, a LiDAR flight was realized on 21 August 2008 by a Leica ALS 50 scanner with an average point density of 5 points / m². For our investigations DSM and a DTM grid of 0.25 m raster width was produced from the raw data. A colour coded hillshade of the LiDAR DSM is given in Fig. 9. 20 cm orthoimages have been calculated from each data set using the LiDAR DTM.

3 Methods

3.1 *Land Cover Classification*

To ensure the objectivity of the comparison, the same training areas for all different cameras were chosen. The training areas were chosen after the criteria by DENNERT-MÖLLER (1983). They had to be

● connected and large enough
● all the pixels in an area need to be contiguous
● homogeneous with an unmixed spectral signature
● be representative for each class
● and spectrally well separable.

The classification method consisted of two steps: a pixel-based maximum likelihood classification (JENSEN 2005) and a decision tree based classification. The maximum likelihood method was used because it showed the best results among other six classification methods for different agricultural scenes in a previuos study (KLONUS & EHLERS 2009). Additionally, a higher objectivity is ensured since it is relatively simple and only a few parameters need to be defined. To avoid an inaccurate classification, weights to each of the classes were added. These weights were the same in all the scenes of all the cameras and were determined using experienced data from other classifications.

The normalized difference vegetation index (NDVI) was added as an additional input parameter for the comparison between DMC and JAS-150 data. The results of the maximum likelihood classification (in the form of a layer) together with the grey value information of the input bands (and the NDVI – if available) were used to build the decision tree.

A decision tree is a hierarchy of rules and consists of different nodes. The first or root node is displayed at the top, connected by successive branches to other nodes. These are similarly connected until a leaf node is reached, which has no further branches. Each leaf node is similar to a class in Tab. 3. The classification of a particular pattern (vector in feature space) begins at the root node. Each node contains a rule, e. g. NDVI > 500. The different branches from the root node correspond to the different possible answers, in this case yes or no. Based descendent on the answer it follows the appropriate branch to a subsequent or descendent node. Therefore the branches must be mutually distinct and exhaustive. The next step is to make the decision at the sub-tree appropriate subsequent node, which can be considered the root of a sub-tree. This way is continued until a leaf node is reached, which has no further rule (DUDA et al. 2001).

To guarantee a high objectivity of the classification the settings for the decision tree were extracted automatically from the training areas using the mean and standard deviations of the pixel values in these areas. Overall, fourteen different classes were distinguished for this classification (see Tab. 3). The images were visually assessed and quantitatively analysed using 255 randomly chosen points in the classified images. Then the points were compared to field data, and producers' and users' accuracy and the kappa coefficient were calculated. Classes that had less than five points were not included in the analysis (see also Tab. 2).

3.2 *Tree Species Classification*

Variables Derived from Remotely Sensed Information

The extraction of tree area and classification of tree species is based on logistic regression models (for details see, e. g., HOSMER & LEMESHOW 1989). As explanatory variables several geometric and spectral signatures were derived from the remote sensing data using standard digital image processing methods as described in (GONZALES & WOODS 2002).

A detailed extraction of geometric and spectral explanatory variables derived from airborne remote sensing data is described in WASER et al. (2007 and 2008a). The explanatory variables used in this study consist of four commonly used geometric parameters derived from the LiDAR DSMs (slope, curvature, and two local neighbourhood functions: rate of change in slope for each cell and assessment of topographic position). For further details, see BURROUGH (1986).

Based on experiences made in WASER et al. (2008b) as spectral input variables we produced for each data set: four original bands (RGB and NIR) of ADS40-2nd, DMC and JAS-150, Ultracam-X (only 3 bands RGB were available); the 3 ratios of each RGB band divided by the sum of the corresponding three bands; and the three colour transformations from RGB to IHS into the 3 channels intensity (I), hue (H), and saturation (S). In total we have derived ten spectral input variables from each of the ADS40-2nd, DMC and JAS-150 data sets and 9 from the Ultracam-X where no NIR channel was available for this study.

Image Segmentation

Homogenous image segments of individual tree crowns or tree-clusters are needed to extract the tree area and to classify tree species (see below). The four orthoimages were therefore subdivided into patches by a multi-resolution segmentation using the Definiens 7.0 software (BAATZ & SCHÄPE 2000). The RGB bands are used as input data with the LiDAR DSMs providing additional geometric information (height and slope). Segmentation was iteratively optimized using several levels of detail

and an adapted to shape and compactness parameters.

Finally, the means and standard deviations of the remotely sensed explanatory variables, the variables derived from them were calculated for each segment.

Tree Cover

The extraction of the tree area is a required input in classification of the tree species approach. Tree canopy and non-tree area masks were generated in five steps. First, a digital canopy height model (CHM) was produced subtracting the LiDAR DTM from the DSM. In a second step, pixels with CHM values > 2 m were used to extract potential tree areas. Then four shadow masks were empirically generated using the spectral information (ratio of channels) from the four input orthoimages. In a fourth step, non-tree objects, e. g. buildings, roofs, artefacts in the CHMs were removed using NDVI values (ADS40-2nd, DMC, JAS-150) or ratio of red / green bands (Ultracam-X) information (curvature) about the image segments (e. g. segments on buildings have lower curvature values and ranges). These four steps resulted in a canopy cover per data set (four in total) providing discrete tree / non-tree data.

Then in a fifth step, based on these canopy covers, four fractional tree covers were produced using logistic regression and the four topographic variables from the CHM as described above, with a probability for each image segment that it belongs to the class "tree". The probability (P) for each pixel that belongs to the class "tree" ranges between 0 and 1. Segments with a tree probability of 0.5 or more were assigned to the class "tree", the others to the class "non-tree". To validate the method, a similar regression was applied to segments with our ground truth data with a tree or non-tree sample unit by at least 50 %. The validation consisted of a 5-fold cross-validation of the logistic model.

Tree Species Classification

The tree species were classified within the tree covers (for each data set) using logistic regression models. Prior to modelling the tree species for the whole area, the variables were selected empirically using the image segments of each data set with species assignments. The best model runs were obtained using the variables derived from the IHS transformations of the original image bands (means and standard deviations) and the NIR bands (if available). As output, probabilities for each tree species within an image segment were obtained for each data set. The following eight tree species were modeled: ash, beech, maple, Norway spruce, oak, poplar, Scots pine, and willow.

4   Results and Discussion

4.1 *Visual Analysis*

Prior to image classification of test site 1 a visual analysis was performed to detect similar training areas. For interpretation purposes the images of the different sensors are displayed
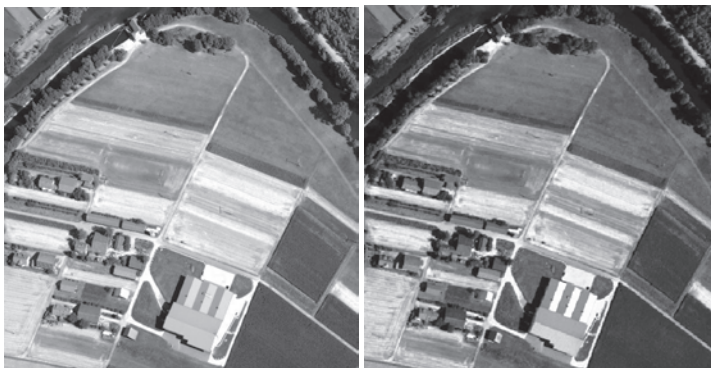

Fig. 3: Red band of DMC (left) and RMK-Top15 (right).

Fig. 4: Red band of Quattro DigiCAM (left) and JAS-150 (right).

in the red band (Figs. 3–5). The red band was chosen since only the red and green bands were available for all sensors. At first glance, visual analysis revealed that most of the images of the different cameras have a similar quality and the different field crops and land cover classes could be easily extracted.

However, the missing atmospheric correction is clearly visible in the RMK-Top15 and the JAS-150 images. The position of the sun during image acquisition was east of the scenes and the effects can be clearly seen on the roof of the big farmyard at the bottom.

Some differences in the appearance of the vegetation are also visible in the field in the north of the big farmyard. While the contrast between the different fields in images from DMC and RMK-Top15 is high, images from Ultracam-X are characterized by a lower contrast. Additionally to the atmospheric differ-ences, differences in contrast might be caused by the different phenological state due to the different dates of image acquisition.

4.2 *Thematic Classification*

The overall classification accuracies for each sensor are summarized in Tab. 2. Figs. 6–8 show the examples of the land cover classifications based on the different sensors. With variations of the kappa coefficient of only 0.15 (Tab. 2) the quantitative results confirmed what the visual assessments suggested (cf. Figs. 3–5), that all cameras performed simi-larly.

The relatively low kappa coefficients are caused by different factors: (a) The application of the same method to all different images, (b) different weather conditions during the re-cording of the images, (c) phenological differ-ences between the images and (d) bi-direc-tional reflectance distribution function (BRDF)-related problems such as the natural in-field variations or the missing atmospheric corrections. Atmospheric corrections were not applied since they are hardly used in praxis. A consideration of the BRDF may lead to better results since the final greyvalues in the image strongly depend on the position of the sun and the position of the observer relative to the sun (DEMIRCAN et al. 2009). To reduce these ef-fects, an attempt was made to use only one im-age per classification. Image mosaics were solely used if the single images were smaller than the study area.

Fig. 5: Red band of Ultracam-X.

Tab. 2: Fourteen thematic classes (all data except of Cohen's kappa coefficient (*K*) is given in %, for cells with --- less than 5 reference points were available).

Class	RMK-Top15 (RGN)	DMC (RGB)	DMC (RGBN)	JAS-150 (RGB)	JAS-150 (RGBN)	Quattro Digi-CAM (RGB)	Ult-racam-X (RGB)
Fallow ground	97.05	60.36	79.69	69.23	81.86	74.03	85.08
Water with Algae	---	---	60.00	80.00	75.00	62.50	---
Grassland	83.32	69.46	74.30	64.65	74.74	77.10	75.72
Potato	---	---	---	---	---	---	---
Corn	---	53.70	25.75	---	60.72	54.17	---
Shadow	66.67	80.77	78.25	84.45	80.98	77.27	62.22
Quarry	65.39	42.43	53.34	12.70	80.81	62.22	57.15
Stubble field	91.67	53.62	82.02	90.45	85.06	94.15	63.05
Streets	34.09	71.47	75.56	29.83	41.67	32.15	66.97
Buildings	49.09	58.93	59.09	59.53	51.76	75.00	75.00
Forest	69.09	81.38	74.80	78.90	79.76	70.38	69.61
Water	96.42	67.33	92.04	92.13	94.77	76.51	88.99
Vineyard	---	58.34	---	---	---	62.50	66.67
Sugar beets	78.57	63.64	62.50	62.92	38.57	71.43	67.50
K	0.66	0.53	0.63	0.62	0.68	0.68	0.58

Figs. 6–8 clearly show that most of the grassland are correctly classified. However, in some parts of the RMK-Top15 and JAS-150 images this class is mixed with pixels of sugar beets. The characteristics of the river Enz are clearly visible in all classified scenes and only the size of the area of algae varies. Especially in the JAS-150 images most of the algae are classified as forest. Further problems occurred in separating sugar beets from grassland and corn from forest.

The detection of corn shows a relatively low accuracy. In one corn field no single pixel has been classified as corn and distinction between fallow and stubble fields was not always possible using the JAS-150, RMK-Top15 and Ultracam-X images. The real distribution of stubble or fallow lands could not accurately be determined due to the time differences between the flights and the lack of information on the field crops of each day. Generally, the accuracy for these two classes is about 80 %. The misclassified pixels mostly belong to other crops, and only the JAS-150 images show

misclassified pixels which corresponded to artificial structures such as stones or buildings.

Another problem occurred when classifying the vineyards. The usage of 20 cm resolution images did not absolutely guarantee pure pixels of vineyards for the trainings areas. Therefore the overall accuracy of the classification is reduced by the vineyard class. Nearly 5 % better results are obtained when performing a classification without vineyards.

The analysis of the shadow class has been separated into three types: shadows over water, shadow in vegetation and shadows in settlements. The RMK-Top15 detected most of the shadows in vegetation as water with high amount of algae; the usage of this sensor also generates problems with shadows over water because the majority was not detected. The extraction of shadows in vegetation and water was good using the images from DMC and Quattro DigiCAM. In the Ultracam-X images most of the shadows in settlements are classified as water. The best results are again obtained for DMC and Quattro DigiCAM. Since
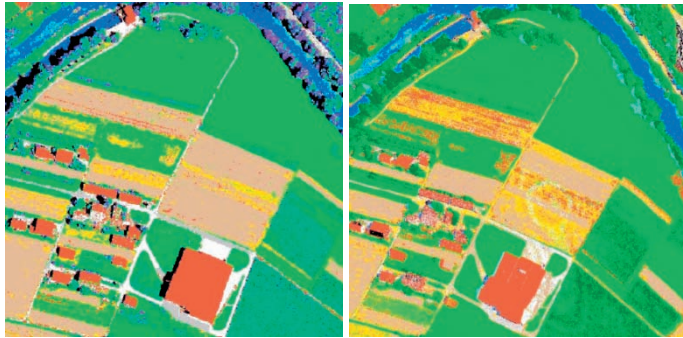
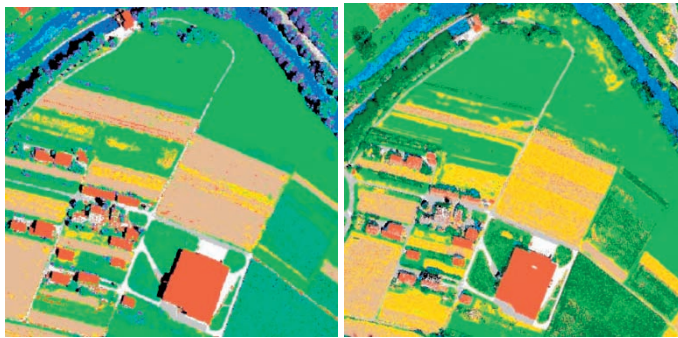**Fig. 6:** Classification results for Quattro DigiCAM (left) and RMK-Top15 (right).

Fig. 7: Classification results for DMC (left) and Ultracam-X (right).

Tab. 3: The 14 thematic classes of the land cover classification approach.

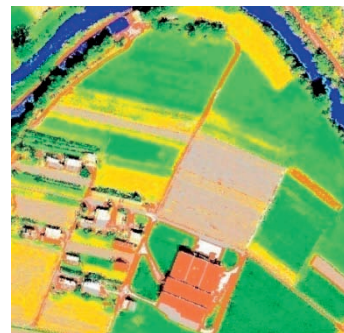| Class	Color	Class	Color
Fallow ground		Stubble field	
Water with algae		Streets	
Grassland		Buildings	
Potato		Forest	
Corn		Water	
Shadow		Vineyard	
Quarry		Sugar beets	

Fig. 8: Classification results for JAS-150.

the quarry stone class is mixed with the street class in all images low accuracies are obtained for both with the exception of the DMC classification where an accuracy of over 70 % is obtained. In the Quattro DigiCAM images the marks on the streets and the borders of the streets are mostly classified as quarry stone.

In the JAS-150 images especially the larger streets are extracted as buildings whereas the small streets are predominantly correctly classified. In the RMK-Top15 images many of the street pixels are classified as quarry stone and fallow field. Generally, buildings can be visually separated from the remaining classes. Misclassified buildings in the JAS-150 images are mostly due to strong light reflections on one site of the roofs which in turn are caused by the low altitude of the sun. The best results

are obtained using the images from Quattro DigiCAM and Ultracam-X.

Since only one potatoe field exists in test site 1 only few reference points were allocated to this class. The visual inspection shows, that this class has a low accuracy and more than 40 % of the pixels are classified as other crop types. High accuracies are obtained for the forest class by all sensors. The Quattro Digi-CAM scene shows a lot of corn pixels in the final result. Best results for this class are obtained when using the DMC and the JAS-150 images. On the other hand, in all images most of the corn pixels have been classified as forest. The relatively high accuracy obtained by the RMK-Top15 images is due the additional usage of the near infrared band.

4.3 *Tree Species Classification*

The modelled tree covers were cross-validated using a patch-to-patch comparison to the ground truth data (120 tree and non-tree samples), i. e. segments overlapping at least 50 % with a tree or non-tree sample unit. Tab. 4 summarizes the correspondence between the randomly sampled tree / non-tree samples and the modelled tree covers for each of the four datasets of this study. The accuracy of the classified trees was generally high in all four data sets. The fact that the geometric parameters alone almost suffice for the generation of the tree covers underlines the importance of the LiDAR DSM quality. An example of the CHM and the tree cover classification is given in Fig. 9.

Tab. 4: Correctly classified tree / non-tree segments (%) and Cohen's kappa coefficient (K).

	ADS40-2nd	DMC	JAS-150	Ultracam-X
Tree segments	524	521	533	512
Non-tree segments	454	465	432	448
Correct (%)	99	99	99	99
K	0.95	0.96	0.95	0.95

Tree probability ☐ 95-100% ☐ 90-95% ■ < 90%

☐ maple ☐ oak ■ poplar ☐ pine
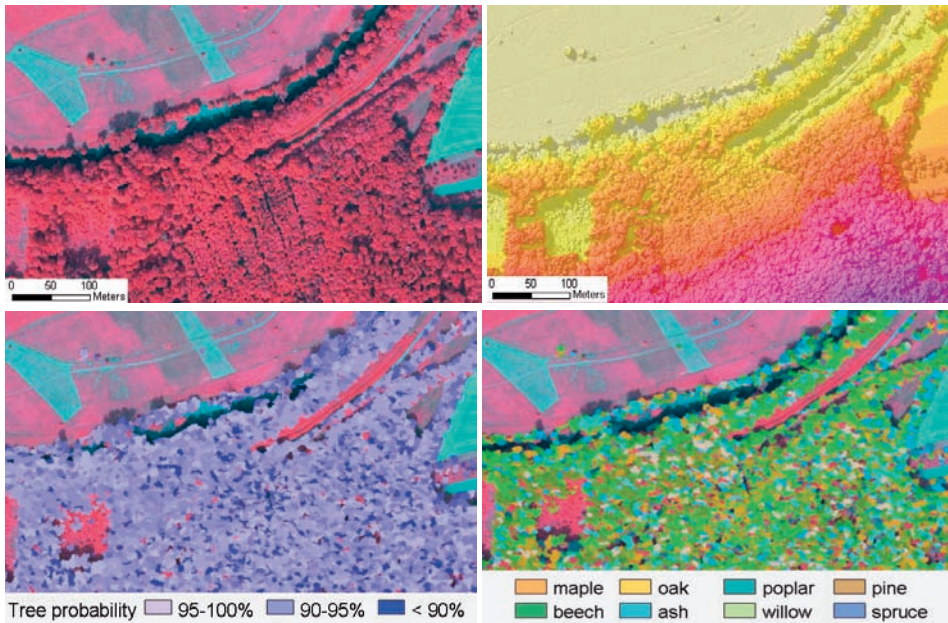☐ beech ☐ ash ☐ willow ☐ spruce

Fig. 9: Top left: ADS40-2nd CIR orthoimage of a part of test site 2; top right: colour-coded hillshade of LiDAR DSM, classification of tree probabilities (bottom left) and tree species (bottom right).

In order to validate the classification of the main tree species, the reference tree data was assigned to the corresponding image segments using ArcGis 9.3.1. Each of the 240 delineated reference tree species was assigned to an image segment if the overlapping area of the specific species was at least 10 %. If this was the case, for each segment the tree species with

Tab. 5: Confusion matrices for tree species classification using different data sources, proportion of correctly classified trees (prop. corr. %) of different tree species, overall accuracy (ov. acc. %), and Cohen's kappa coefficient (K). The number of tree segments used varies in each model; in the segmented DMC image 456 tree segments were assigned, 500 in the ADS40-2nd, 452 in the JAS-150, and 462 in the Ultracam-X image.

Field	Classified as								Ov. acc. %	K
	Maple	Beech	Ash	Poplar	Oak	Willow	Spruce	Pine		
DMC										
Maple	6	0	7	3	0	0	0	0		
Beech	0	**89**	19	2	0	0	0	0		
Ash	0	15	**79**	3	0	0	0	0		
Poplar	0	1	3	**72**	0	0	0	0		
Oak	0	0	0	0	**4**	0	0	0		
Willow	0	0	0	0	0	**69**	0	0		
Spruce	0	0	0	0	0	0	**58**	0		
Pine	0	0	0	0	0	0	0	**26**		
Prop. corr.(%)	38	71	63	86	100	100	100	100	**88.4**	**0.86**
ADS40-2nd										
Maple	**8**	5	3	0	0	0	0	0		
Beech	6	**109**	10	1	0	0	0	0		
Ash	6	22	**71**	2	1	1	0	0		
Poplar	5	2	2	**52**	0	4	0	0		
Oak	0	0	2	1	**3**	0	0	0		
Willow	2	3	1	2	0	**67**	0	0		
Spruce	0	0	0	0	0	0	**74**			
Pine	0	0	0	0	0	0		**35**		
Prop. corr. (%)	23	69	59	73	43	84	100	100	**83.8**	**0.81**
JAS-150										
Maple	**3**	9	1	0	0	0	0	0		
Beech	1	**97**	11	1	0	1	2	0		
Ash	0	31	**49**	4	0	1	1	0		
Poplar	0	3	3	**59**	0	2	0	0		
Oak	0	0	0	0	**5**	0	0	0		
Willow	0	0	0	0	0	**67**	1	0		
Spruce	0	2	0	0	0	0	**65**	0		
Pine	0	0	0	0	0	0	0	**33**		
Prop. corr.(%)	21	61	41	82	100	94	93	100	**80.3**	**0.76**
Ultracam-X										
Maple	**1**	7	4	0	0	3	1	2		
Beech	1	**77**	18	4	0	0	9	1		
Ash	1	20	**73**	2	0	4	2	1		
Poplar	0	1	3	**66**	0	3	0	0		
Oak	0	5	0	0	**2**	0	0	0		
Willow	0	3	1	9	0	**53**	1	1		
Spruce	0	5	0	1	0	1	**47**	1		
Pine	0	2	0	1	0	0	0	**25**		
Prop corr.(%)	5	53	50	73	29	67	70	74	**74.1**	**0.69**

the most overlapping area was assigned. The classified tree species were then cross-validated (5 times) using a segment-to-segment comparison on the delineated reference tree data per sensor. To test the 'robustness' of the methods and to see whether consistent results could be achieved, the training and testing samples were exchanged. Tab. 5 shows the four confusion matrices for tree species classification. An example of the classified tree species based on the ADS40-2nd input data are depicted in Fig. 9.

Tab. 5 shows that overall classification accuracies are generally high for each input data set and variations of the kappa coefficient lay within 17 %. The model based on DMC data produced highest accuracies for all tree species. At first glance, visual assessments of the classifications suggest that all cameras performed quiet similarly and that the agreements in most parts of the site are good. Some differences are visible between deciduous and coniferous trees and within deciduous tree species. Coniferous tree species are generally better classified than deciduous trees when using the DMC, ADS40-2nd and JAS-150 data sets. The lower accuracies of coniferous trees in the Ultracam-X data set are obvious and most probably due to the missing NIR channel. The analysis showed that the results for deciduous trees are generally less accurate. Oaks as a non-dominant tree species vary from 29 % (Ultracam-X) to 100 % (DMC, JAS-150) correctly classified, however this classification is based on very few samples. Second best results are obtained for poplar and willow (67 % to 100 %). Again highest accuracies are obtained from DMC and JAS-150 data. The analysis showed that the classification of maple was the least accurate. Most errors involved maple being misclassified as beech (ADS40-2nd, JAS-150, Ultracam-X) or ash (DMC). Beech is often misclassified as ash (all data sets) or as Norway spruce (Ultracam-X). Visual image inspection showed that old and tall beeches and ashes are often difficult to distinguish since they have a similar structure (opened crowns with tall branches and few leaves) and very often also spectral similarities. Even within species, spectral variability can be large because of illumination and view-angle conditions, openness of trees,
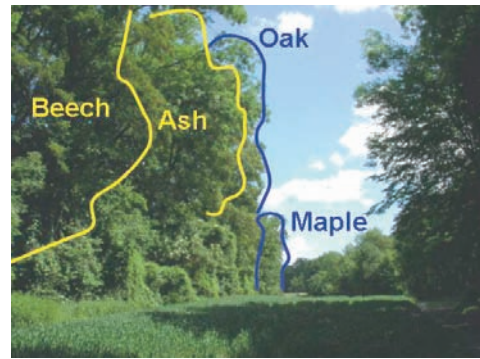

Fig. 10: Illustration to show the problems involved in identifying deciduous trees. Both beech and ash have a similar structure with large partly leaf-less branches, at the background a dominant oak is partly covering a smaller maple which is characterized by having a smaller crown diameter.

natural variability, shadowing effects and differences in crown health.

Spectral separability between species and the variability of trees within species have also been analysed and described in LECKIE et al. (2005). Maples as non-dominant deciduous tree species in this region can be more difficult to identify because they may be short and shaded or obscured by nearby large tree species, or by the merging of close crowns. The field visit and visual stereo-image interpretation revealed that maples are often not grouped, have smaller crowns and are therefore partly covered by each other or by larger trees. Fig. 10 illustrates this situation.

5 Conclusions and Recommendations

The present study shows the potential and the limits of classifying thirteen land cover and eight tree species classes using newest digital airborne sensors tested in the the DGPF-project. Small variations in classification results are most probably due to phenological differences, different illumination and atmospheric conditions. However, an absolute and clinical one to one comparison between the classification results obtained by the different camera systems was not possible due to the following reasons: 1) the usage of different

bands or band combinations, 2) different dates of image acquisition which causes phenological differences in vegetation growth (especially for cropland), and 3) varying atmospheric conditions (illumination and visibility).

The first approach which uses imagery from the five aerial cameras DMC, RMK-Top15, Quattro DigiCAM, JAS-150 and Ultracam-X produces a similar overall Kappa coefficient, but very different classification accuracies are obtained for the single classes. The classification accuracy is relatively low, but in order to keep the objectivity of the comparison, the first classification approach was not adjusted to the characteristics of each camera. This is planned to be done in the near future. Other reasons for the low accuracy are the weather conditions and BRDF related problems.

The most significant achievement of the second approach is the demonstration that combining the four data sets of ADS40-2nd, DMC, JAS-150, Ultracam-X with logistic regression models to classify tree species has a very high potential to produce meaningful results, especially when supported by the NIR bands. Promising classification results for the main tree species were confirmed with ground information and what can be seen visually on the imagery. Further work is needed to improve distinguishing non-dominant, small and partly covered tree species.

To overcome these problems we suggest atmospheric corrections, and radiometric corrections for future work as the requests and the realisation of the radiometric analyses as a part of the DGPF-project is outlined in SCHÖNERMARK (2010). This also implies BRDF-related problems or investigation of influences of the BRDF in terms of classification accuracy. During the vegetation period only few days (e. g. after precipitation) may change the spectral properties and thus separability of some crops significantly. This problem could be solved and the ground truth could be further improved by collecting more samples and field visits during the image acquisition.

Nevertheless, the experiences of the newest digital airborne sensors made in this study may be of practical interest or serve as a basis for decisions for tasks of environmental agencies, forest inventories or land surveying offices.

References

ALBERTZ, J., 2001: Einführung in die Fernerkundung, Grundlagen der Interpretation von Luft- und Satellitenbildern. – Wissenschaftliche Buchgesellschaft, Darmstadt.

BAATZ, M. & SCHÄPE, A., 2000: Multiresolution Segmentation – an optimization approach for high quality multi-scale image segmentation. – Angewandte Geographische Informationsverarbeitung **XII**: 12–23; Wichmann, Heidelberg.

BAILLY, J.S., ARNAUD, M. & PUECH, C., 2007: Boosting: a classification method for remote sensing. – International Journal of Remote Sensing **28** (7–8): 1687–1710.

BURROUGH, P.A., 1986: Principles of Geographical Information Systems for Land Resources Assessment. – Oxford University Press, New York, USA.

CRAMER, M., 2010: The DGPF-Test on Digital Airborne Camera Evaluation – Overview and Test Design. – This issue.

DEMIRCAN, A., SCHUSTER, R., RADKE, M., SCHÖNERMARK, M. V. & RÖSER, H.P., 2000: Use of a wide angle CCD line camera for BRDF measurements. – Infrared Physics & Technology **41** (1): 11–19.

DENNERT-MÖLLER, E., 1983: Untersuchung zu digitalen multispektralen Klassifizierung von Fernerkundungsaufnahmen mit Beispielen aus den Wattgebieten der deutschen Nordseeküste. – Wissenschaftliche Arbeiten der Fachrichtung Geodäsie und Geoinformatik, Hannover.

DUDA, R.O., HART, P.E. & STORK, D.G., 2001: Pattern classification. – John Wiley & Sons, New York, USA.

EHLERS, M., SCHIEWE, J., ROSSO, P. & KLONUS, S., 2007: Prüfung von Luftbilddaten zweier unterschiedlicher Aufnahmesensoren hinsichtlich eines optimalen Aufnahmesystems zur Erfüllung von Aufgaben von Vermessungs- und Umweltverwaltung für das Landesamt für Natur und Umwelt (LANU). – gi-reports@igf, **9**, Universität Osnabrück.

ERBEK, F.S., ÖZKAN, C. & TABERNER, M., 2004: Comparison of maximum likelihood classification method with supervised artificial neural network algorithms for land use activities. – International Journal of Remote Sensing **25** (9): 1733–1748.

GONZALES, R.C. & WOODS, R.E., 2002: Digital image processing – Second edition; Prentice Hall, Upper Saddle River, NY, USA.

HEINZEL, J.N., WEINACKER, H. & KOCH, B., 2008: Full automatic detection of tree species based on delineated single tree crowns – a data fusion approach for airborne laser scanning data and aer-

ial photographs. – SilviLaser – 8th international conference on LiDAR applications in forest assessment and inventory, 76–85.

HIRSCHMUGL, M., OFNER, M., RAGGAM, J. & SCHARDT, M., 2007: Single tree detection in very high-resolution remote sensing data. – Remote Sensing of Environment **110:** 533–544.

HOLMGREN, J., PERSSON, A. & SODERMAN, U., 2008: Species identification of individual trees by combining high resolution LiDAR data with multi-spectral images. – International Journal of Remote Sensing **29:** 1537–1552.

HONKAVAARA, E., ARBIOL, R., MARKELIN, L., MARTINEZ, L., CRAMER, M., BOVET, S., CHANDELIER, L., ILVES, R., KLONUS, S., MARSHAL, P., SCHLÄPFER, D., TABOR, M., THOM, C. & VEJE, N., 2009: Digital Airborne Photogrammetry – A New Tool for Quantitative Remote Sensing? – A State-of-the-Art Review On Radiometric Aspects of Digital Photogrammetric Images. – Remote Sensing **1:** 577–605.

HOSMER, D.W. & LEMESHOW, S., 1989: Applied logistic regression. – Wiley, New York, USA.

JENSEN, J.R., 2005: Introductory digital image processing: A remote sensing perspective. – Prentice Hall, Upper Saddle River, NY, USA.

KLONUS, S., 2009: Thematische Klassifikation von DMC, RMK, DigiCAM, JAS-150 und UCX-Bildern. – www.ifp.uni-stuttgart.de/dgpf/Stuttgart09/2_4-KLONUS.pdf (17.12.2009).

KLONUS, S. & EHLERS, M., 2009: Additional benefit of image fusion method from combined high resolution TerraSAR-X and multispectral SPOT data for classification. – 29th Earsel Symposium, in press.

KLONUS, S., HAGEDORN, C., EKKEHARD, J., CASTILLO, K., GONZALO, J. & VELEZ, F., 2009: Digitalisierung der Landnutzungserhebungen und erste Klassifikationsergebnisse. – Wissenschaftlich-Technische Jahrestagung der DGPF.

LECKIE, D.G., TINIS, S., NELSON, T., BURNETT, CH., GOUGEON, F.A., CLONEY, E. & KPARADINE, D., 2005: Issues in species classification of trees in old growth conifer stands. – Canadian Journal of Remote Sensing **31** (2): 175–190.

LILLESAND, T.M. & KIEFER, R.W., 1994: Remote Sensing and Image Interpretation – Third Edition; Wiley, New York, USA.

LU, D. & WENG, Q., 2007: A survey of image classification methods and techniques for improving classification performance. – International Journal of Remote Sensing **28** (5): 823–870.

MARKELIN, L., HONKAVAARA, E., PELTONIEMI, J., SUOMALAINEN, J. & AHOKAS, E., 2006: Radiometric Evaluation of Digital Aerial Cameras. – International Achieves of Photogrammetry, Remote Sensing and Spatial Information Sciences **36** (1): 75–80.

ROSSO, P.H., KLONUS, S., EHLERS, M. & TSCHACH, E., 2008: Comparative Properties of Four Airborne Sensors and their Applicability to Land Surface Interpretation. – International Archives of the Photogrammetry, Remote Sensing and Spatial Information Sciences **37** (B1): 545–550.

SCHÖNERMARK VON, M., 2010: Status Report on the Evaluation of the Radiometric Properties of Digital Photogrammetric Airborne Cameras. – This issue.

SCOTT, J.M., HEGLUND, P.J., SAMSON, F., HAUFLER, J., MORRISON, M. & WALL, B., 2002: Predicted species occurrences: issues of accuracy and scale. – Island Press, Covelo, California, USA.

WANG, Z., BOESCH, R. & GINZLER, C., 2007: Color and LiDAR data fusion: Application to automatic forest boundary delineation in aerial images. – International Archives of the Photogrammetry, Remote Sensing and Spatial Information Sciences **36** (1/W51).

WASER, L.T., KÜCHLER, M., ECKER, K., SCHWARZ, M., IVITS, E., STOFER, S. & SCHEIDEGGER, CH., 2007: Prediction of Lichen Diversity in an Unesco Biosphere Reserve – Correlation of high Resolution Remote Sensing Data with Field Samples. – Environmental Modeling & Assessment **12** (4): 315–328.

WASER, L.T., BALTSAVIAS, E., ECKER, K., EISENBEISS, H., GINZLER, C., KÜCHLER, M., THEE, P. & ZANG, L., 2008a: High-resolution digital surface models (DSM) for modelling fractional shrub/tree cover in a mire environment. – International Journal of Remote Sensing **29** (5): 1261–1276.

WASER, L.T., GINZLER, C., KÜCHLER, M. & BALTSAVIAS, E., 2008b. Potential and limits of extraction of forest attributes by fusion of medium point density LiDAR data with ADS40 and RC30 images. – SilviLaser – 8th international conference on LiDAR applications in forest assessment and inventory, 625–634.

Addresses of the Authors:

Dipl. Geograph LARS TORSTEN WASER, Swiss Federal Research Institute WSL Birmensdorf, Airborne Remote Sensing for forest applications, Zuercherstrasse 111, CH-8903 Birmensdorf, Tel.: +41-44-739-22-92, e-mail: lars.waser@wsl.ch.

Dipl. Umweltwiss. SASCHA KLONUS, Prof. Dr.-Ing. MANFRED EHLERS, Universität Osnabrück, Institut für Geoinformatik und Fernerkundung, Barbarastrasse 22b, D-49076 Osnabrück, Tel.: +49-541-969-

3921, -3910, Fax: -3939, e-mail: sklonus@igf.uni-osnabrueck.de, mehlers@igf.uni-osnabrueck.de.

Dr. MEINRAD KÜCHLER, Swiss Federal Research Institute WSL Birmensdorf, Biotopbeurteilung, Zuercherstrasse 111, CH-8903 Birmensdorf, Tel.: +41-44-739-24-67, e-mail: meinrad.kuechler@wsl.ch.

Dr. ANDRAS JUNG, Martin-Luther-Universität Halle-Wittenberg, Institut für Geowissenschaften, Von-Seckendorff-Platz 3–4, D-06120 Halle, Tel.: +49-345-552-6021, Fax: -8228, e-mail: andras.jung@geo.uni-halle.de.